

Diffusion coefficients of phenylbutazone in
supercritical CO₂ and in ethanol

メタデータ	言語: eng 出版者: 公開日: 2014-01-07 キーワード (Ja): キーワード (En): 作成者: Kong, Chang Yi, Watanabe, Kou, Funazukuri, Toshitaka メールアドレス: 所属:
URL	http://hdl.handle.net/10297/7473

1 Diffusion coefficients of phenylbutazone in supercritical CO₂ and in
2 ethanol

3
4 Chang Yi Kong^{a,*}, Kou Watanabe^a and Toshitaka Funazukuri^b

5
6 ^a Department of Applied Chemistry and Biochemical Engineering, Faculty of Engineering,
7 Shizuoka University, 3-5-1 Johoku Naka-ku, Hamamatsu 432-8561, Japan

8 ^b Department of Applied Chemistry, Faculty of Science and Engineering , Chuo University,
9 Kasuga 1-13-27, Bunkyo-ku, Tokyo, 112-8551, Japan.

10
11 * Corresponding author. Tel.: +81 53 478 1174; fax: +81-53 478 1174.

12 *E-mail address:* tcykong@ipc.shizuoka.ac.jp (C.Y. Kong).

13

14 **Abstract**

15 The diffusion coefficients D_{12} of phenylbutazone at infinite dilution in supercritical CO₂ were
16 measured by the chromatographic impulse response (CIR) method. The measurements were carried
17 out over the temperature range from 308.2 to 343.2 K at pressures up to 40.0 MPa. In addition, the
18 D_{12} data of phenylbutazone at infinite dilution in ethanol were also measured by the Taylor
19 dispersion method at 298.2 to 333.2 K and at atmospheric pressure. The D_{12} value of
20 phenylbutazone increased from $4.45 \times 10^{-10} \text{ m}^2 \text{ s}^{-1}$ at 298.2 K and 0.1 MPa in ethanol to about 1.43
21 $\times 10^{-8} \text{ m}^2 \text{ s}^{-1}$ at 343.2 K and 14.0 MPa in supercritical CO₂. It was found that all diffusion data of
22 phenylbutazone measured in this study in supercritical CO₂ and in ethanol can be satisfactorily
23 represented by the hydrodynamic equation over a wide range of fluid viscosity from supercritical
24 state to liquid state with average absolute relative deviation of 5.4% for 112 data points.

25

26

27

28 *Keywords:* Supercritical carbon dioxide, Diffusion coefficient, Phenylbutazone, Chromatographic
29 impulse response method, Taylor dispersion method, Pharmaceutical

30 **1. Introduction**

31 Supercritical fluid is a substance whose temperature and pressure are simultaneously above its
32 critical point. Processing materials with supercritical fluid is a proven and industrially applicable
33 technology. Supercritical CO₂ is the most widely used in research studies and industrial applications.
34 It is non-toxic, non-flammable, chemically inert and inexpensive. Furthermore, it is a green and
35 versatile solvent having near ambient critical temperature, and promising alternative to noxious
36 organic solvents. The commercial application of combination of pharmaceutical and supercritical
37 CO₂ is one of interesting research areas with significant potential [1,2]. To design and improve new
38 supercritical process, it is needed to understand the fundamental information of the supercritical
39 system. Estimation of mass transfer properties in supercritical fluid is required the diffusion data.
40 Phenylbutazone, is an active pharmaceutical ingredient, which is used primarily in non-steroidal
41 anti-inflammatory pharmaceutical that also possesses antipyretic and analgesic effects.
42 Unfortunately, the diffusion data [3-7] are few for pharmaceutical in supercritical CO₂, and no data
43 are available in literature for the system of phenylbutazone and CO₂. The objective of this work was
44 to measure the diffusion coefficients D_{12} of phenylbutazone at infinite dilution in supercritical CO₂
45 by the chromatographic impulse response (CIR) method. And then, the D_{12} data of phenylbutazone
46 in ethanol were also measured by the Taylor dispersion method. Furthermore, the validity of the
47 hydrodynamic equation D_{12}/T as a function of fluid viscosity was examined for all diffusion data
48 measured in this study.

49

50 **2. Theory**

51 The theories for the CIR and the Taylor dispersion methods have been described in detail
52 previously [8-10], in here, briefly described. When a tracer species is pulse-injected into a fully
53 developed laminar flow in a cylindrical column, the cross-sectional average concentration $C(t)$ can
54 be described as follows:

$$\begin{cases}
C(t) = \left(\frac{m}{\pi R^2} \right) \frac{1}{(1+k)(4\pi Kt)^{1/2}} \exp \left\{ -\frac{(L-u_0t/(1+k))^2}{4Kt} \right\} \\
K = \frac{D_{12}}{1+k} + \frac{1+6k+11k^2}{(1+k)^3} \frac{R^2 u_0^2}{48D_{12}} \\
k = \frac{u_0}{u} - 1
\end{cases} \quad (1)$$

56 where t is the time, m the amount of solute injected ($= \pi R^2 u_0 \int_0^\infty C(t) dt \equiv \pi R^2 u_0 \times (\text{peak area})$), R
57 the radius of diffusion column, L the distance, u_0 the average velocity of fluid, and D_{12} the infinite
58 dilution binary diffusion coefficient of the solute. The D_{12} value can be determined by minimizing
59 the root-mean-square (rms) fitting error ε , defined by Eq. (2).

$$\varepsilon = \left(\frac{\int_{t_1}^{t_2} (C_{\text{meas}}(t) - C(t))^2 dt}{\int_{t_1}^{t_2} (C_{\text{meas}}(t))^2 dt} \right)^{1/2} \quad (2)$$

61 where t_1 and t_2 correspond to the times at the front and latter 10% peak heights, respectively, of the
62 measured response curve $C_{\text{meas}}(t)$. The authors [9] evaluated that the ε values less than 1% were a
63 good fit, and those less than 3% were an acceptably good fit. Note that u_0 is needed to obtain
64 experimentally for the CIR method, while it is not required for the Taylor dispersion method.

65

66 3. Experimental

67 3.1. Apparatus and procedure

68 The diffusion coefficients of phenylbutazone were measured by the CIR and Taylor dispersion
69 methods similar to that in the previous study [10]. A polymer-coated capillary open column
70 (UACW-15W-1.0F, the Frontier Laboratories Ltd., Japan, polymer thickness of 1 μm , $R = 0.265$
71 mm, $L = 16.218$ m, and $R_{\text{coil}} = 310$ mm, where R_{coil} is the coil radius of diffusion column) and a
72 non-coated capillary open column (bright annealed 316 Stainless-steel, GL Sciences Inc., Japan, $R =$
73 0.416 mm, $L = 16.634$ m, and $R_{\text{coil}} = 315$ mm) were employed as diffusion column in the CIR

74 method and the Taylor dispersion method, respectively. The diffusion column was immersed
75 horizontally in the water bath (T-105, Thomas Kagaku Co., Ltd., Japan). The pressure of the system
76 was controlled by a syringe pump (260D, ISCO, USA) and a back pressure regulator (Model
77 SCF-Bpg/M, JASCO, Japan). A packed column was installed upstream at the regulator to stabilize
78 the pressure. After the prescribed measurement conditions such as temperature, pressure, and flow
79 rate of fluid had become constant, the system was held under the same conditions for at least a
80 further two hours . Then, a pulse of phenylbutazone predissolved in ethanol was loaded through an
81 injector (Model 7520, 0.5 μ L, Rheodyne, USA) into the fluid flowing. The response curves were
82 monitored with a UV-Vis multi-detector (Model MD-1510, JASCO, Japan). Only a single pulse
83 was injected for each measurement in this study.

84

85 *3.2. Experimental conditions*

86 Phenylbutazone (molecular formula: $C_{19}H_{20}N_2O_2$, molecular weight: 308.37) with purity 99%
87 and ethanol with 99.5% were purchased from Wako, Japan. CO_2 with purity higher than 99.95%
88 was obtained from Air Gases Tokai Ltd., Japan.

89 The measurements for D_{12} were carried out by the CIR method for phenylbutazone at 308.15,
90 313.15, 318.15, 323.15, 333.15, 343.15 K and pressures from 8.50 to 40.00 MPa in supercritical
91 CO_2 . In addition the D_{12} values of phenylbutazone in ethanol were also measured by the Taylor
92 dispersion method at 298.15, 303.15 308.15, 313.15, 318.15, 323.15, 328.15, 333.15 K and at
93 atmospheric pressure. At least three measurements were carried out for a given temperature and
94 pressure, and the average value of the measurements was considered to be the D_{12} .

95

96 **4. Results and Discussion**

97 *4.1. Effects of wavelength, secondary flow and injected amount*

98 Fig. 1 shows the effects of absorption wavelength on (a) absorbance of the peak top of a
99 response curve A_{max} , (b) $A_{max}/(u_0 \times \text{peak area})$, (c) D_{12} and (d) ε for phenylbutazone in supercritical

100 CO₂ at 313.15 K and 11.00 MPa measured by the CIR method. The response curves were measured
101 at wavelengths from 200 to 300 nm at increments of 1 nm for each run. It was found that the
102 absorbance intensities measured were lower than 0.2 AU. And the values of $A_{\max}/(u_0 \times \text{peak area})$ for
103 the whole wavelength were constant, which evidences the linearity of the detector used in this study.
104 Furthermore, the determined D_{12} values were almost constant except for the longer wavelengths
105 (>290 nm) with lower A_{\max} values. And the ε values showed lower values with less than 1% when
106 wavelengths were lower than 290 nm. In this study all D_{12} values were determined from the
107 response curves measured at 240 nm.

108 Fig. 2 represents the effects of CO₂ flow rate on D_{12} of phenylbutazone in supercritical CO₂ at
109 240 nm, 313.15 K and 11.00 MPa measured by the CIR method, together with the ε . The ε values
110 for all data are lower than 1%, however the D_{12} values are affected by the flow rate due to the
111 secondary flow caused by column coiling when $DeSc^{1/2} > 10$, where the Dean number $De =$
112 $(2Ru_0\rho/\eta)(R/R_{\text{coil}})^{1/2}$, the Schmidt number $Sc = \eta/(\rho D_{12})$, the CO₂ density ρ was obtained from the
113 literature [11,12], and the CO₂ viscosity η was from Fenghour et al. [13]. The leveled off value in
114 Fig. 2(a) is adjudged to be the intrinsic D_{12} value. Note that the effect of the secondary flow was
115 evaluated to be less than 1% in terms of the value of the moment when $DeSc^{1/2} < 8 \sim 9.5$ for the
116 measurements by the CIR method [14] and when $DeSc^{1/2} < 8$ for the measurements by the Taylor
117 dispersion method [8]. All measurements were made at $DeSc^{1/2} < 8$ in this study.

118 Fig. 3 plots the effects of the injected amounts m of phenylbutazone on (a) A_{\max} , (b) $u_0 \times (\text{peak}$
119 $\text{area})$, (c) D_{12} and (d) ε measured by the CIR method in supercritical CO₂ at 240 nm, 313.15 K and
120 11.00 MPa. Six difference solutions of phenylbutazone in ethanol over the wide range of the solute
121 concentrations (3.48×10^{-5} , 3.48×10^{-4} , 2.00×10^{-3} , 3.48×10^{-3} , 1.00×10^{-2} and 3.48×10^{-2} g mL⁻¹) were
122 used. Correspondingly the injected amounts of phenylbutazone were 5.64×10^{-5} , 5.64×10^{-4} ,
123 3.24×10^{-3} , 5.64×10^{-3} , 1.62×10^{-2} and 5.64×10^{-2} μmol , respectively. As shown in Fig. 3(b), the
124 values of $u_0 \times (\text{peak area})$ are proportional to m with the slope of about 1. For the injected amounts
125 from 5.64×10^{-5} to 5.64×10^{-2} μmol , all D_{12} values are nearly constant, as observed from Fig. 3(c),

126 and the ε values are lower than 3%. In this study all measurements were carried out with 3.48×10^{-3}
127 g mL⁻¹ ethanol solution of phenylbutazone.

128

129 4.2. Diffusion measured by the CIR method

130 The effect of pressure on D_{12} of phenylbutazone measured by the CIR method in supercritical
131 CO₂ is presented in Fig. 4 and the D_{12} data are listed in Table 1. The D_{12} data were measured
132 isothermally as a function of pressure from 8.50 to 40.00 MPa at 308.15, 313.15, 318.15, 323.15,
133 333.15 and 343.15 K. Note that only the D_{12} data whose ε values were less than 1% were adopted
134 for all measurements in this study. It was observed that the D_{12} values simply decreased with
135 increasing pressure and decreasing temperature, and then the slopes gradually decreased. The
136 influence of pressure on D_{12} was less significant at higher pressures. This behavior has been
137 reported in recent studies [15-31]. On the other hand, the higher pressure sensitivity of D_{12} in the
138 low pressure range can be found, which is probably due to significantly changes in density and
139 viscosity in this region. As has been seen, the D_{12} data can be represented by a simple empirical
140 correlation with temperature and pressure (Eq. (3)) with the average absolute relative deviation
141 (AARD) of 2.8% for 104 data points, while the correlation depends on the system studied.

$$142 \quad D_{12} = 5.92 \times 10^{-9} - 7.51 \times 10^{-12} T - \frac{8.49 \times 10^{-7}}{P} + 2.89 \times 10^{-9} \frac{T}{P} \quad (3)$$

$$143 \quad \text{AARD} = \frac{1}{N} \sum_{i=1}^N \left| \frac{D_{12,i,\text{crl}} - D_{12,i,\text{meas}}}{D_{12,i,\text{meas}}} \right| \times 100\% \quad (4)$$

144 where D_{12} , T and P are in m² s⁻¹, K and MPa, respectively, N is the number of experimental points,
145 and $D_{12, i,\text{crl}}$ and $D_{12, i,\text{meas}}$ are the correlated and measured data, respectively. Although the Eq. (3) is
146 in excellent agreement with the D_{12} data in the higher pressure region, which also can be seen in
147 literature [24,26-29], there is a significant deviation from the experimental data in the lower
148 pressure region at each constant temperature.

149

150 4.3. Diffusion measured by the Taylor dispersion method

151 The effect of temperature on D_{12} of phenylbutazone measured by the Taylor dispersion method
152 in ethanol at 298.15, 303.15, 308.15, 313.15, 318.15, 323.15, 328.15 and 333.15 K is presented in
153 Fig. 5 and the D_{12} data are shown in Table 2. The D_{12} data were measured isobarically as a function
154 of temperature at atmospheric pressure. The D_{12} values increased with increasing temperature at
155 constant pressure. And a high temperature dependence on D_{12} can be observed.

156

157 4.4. Predicting all data

158 Fig. 6 shows D_{12}/T as a function of fluid viscosity η for all D_{12} data of phenylbutazone in
159 supercritical CO₂ measured by the CIR method and in ethanol measured by the Taylor dispersion
160 method in this study. Note that the ethanol viscosities were obtained from the literature [32]. The
161 data can be represented with straight lines given by Eq. (5).

$$162 \frac{D_{12}}{T} = \alpha \eta^\beta \quad (5)$$

163 where α and β are parameters, which are specific to the system of a solute and a fluid. The validity
164 of the correlation in Eq. (5) on the basis of the hydrodynamic approach has been demonstrated for
165 various compounds in supercritical CO₂ [15-23,25,30,31], in organic solvents [33,34] and mixture
166 [35] of supercritical CO₂ and hexane. It was found that all data for the two studied systems of
167 phenylbutazone in CO₂ and phenylbutazone in ethanol also can be represented by Eq. (5). We
168 obtain $D_{12}/T = 2.346 \times 10^{-15} \eta^{-0.955}$ with AARD of 5.4% for 112 data points, where D_{12} , T and η are in
169 m² s⁻¹, K and Pa s, respectively.

170

171 5. Conclusion

172 Infinite dilution binary diffusion coefficients of phenylbutazone in supercritical CO₂ at 308.15,
173 313.15, 318.15, 323.15, 333.15, 343.15 K and 8.50 to 40.00 MPa were measured by the CIR
174 method. In addition the D_{12} data of phenylbutazone in ethanol were measured at 298.15, 303.15,

175 308.15, 313.15, 318.15, 323.15, 328.15, 333.15 K and atmospheric pressure by the Taylor
176 dispersion method. The values of D_{12} for phenylbutazone were determined by fitting the response
177 curve calculated to that measured experimentally. It was found that the D_{12} increased from $4.447 \times$
178 $10^{-10} \text{ m}^2 \text{ s}^{-1}$ at 298.15 K and 0.1 MPa in ethanol to $1.434 \times 10^{-8} \text{ m}^2 \text{ s}^{-1}$ at 343.15 K and 14.00 MPa in
179 supercritical CO_2 . All experimental data were able to be correlated with the hydrodynamic equation
180 D_{12}/T as a function of fluid viscosity with a wide viscosity range (3.232×10^{-5} to $1.113 \times 10^{-3} \text{ Pa s}$)
181 from supercritical to liquid state, and the results showed a good agreement between the correlated
182 results and the experimental data with AARD of 5.4% for 112 data points.

183

184

185

186

187 **Acknowledgements**

188 The authors are grateful to the Ministry of Education, Sports, Culture, Science and Technology
189 of Japan (#22360325) for financially supporting this work.

190

191 **References**

- 192 [1] I. Pasquali, R. Bettini, F. Giordano, *Adv. Drug Delivery Rev.* 60 (2008) 399-410.
- 193 [2] A. Taberero, E.M. Martín del Valle, M.A. Galán, *Chem. Eng. Processing* 60 (2012) 9-25.
- 194 [3] K.K. Liong, P.A. Wells, N.R. Foster, *J. Supercrit. Fluids* 4 (1991) 91-108.
- 195 [4] J.J. Suárez, I. Medina, J.L. Bueno, *Fluid Phase Equilib.* 153 (1998) 167-212.
- 196 [5] T. Funazukuri, C.Y. Kong, S. Kagei, *J. Chromatogr. A* 1037 (2004) 411-429.
- 197 [6] I. Medina, *J. Chromatogr. A* 1250 (2012) 124-140.
- 198 [7] C.Y. Kong, T. Funazukuri, S. Kagei, G. Wang, F. Lu, T. Sako, *J. Chromatogr. A* 1250 (2012)
199 141-156.
- 200 [8] A. Alizadeh, C.A. Nieto de Castro, C.A. Wakeham, *Int. J. Thermophys.* 1 (1980) 243-284.

- 201 [9] C.Y. Kong, T. Funazukuri, S. Kagei, J. Chromatogr. A 1035 (2004) 177-193.
- 202 [10] C.Y. Kong, T. Funazukuri, S. Kagei, J. Supercrit. Fluids 44 (2008) 294-300.
- 203 [11] K.S. Pitzer, D.R. Schreiber, Fluid Phase Equilib. 41 (1988) 1-17.
- 204 [12] R. Span, W. Wagner, J. Phys. Chem. Ref. Data 25 (1996) 1509-1595.
- 205 [13] A. Fenghour, W.A. Wakeham, V. Vesovic, J. Phys. Chem. Ref. Data 27 (1998) 31-44.
- 206 [14] T. Funazukuri, C.Y. Kong, S. Kagei, Fluid Phase Equilib. 59 (2004) 3029-3036.
- 207 [15] T. Funazukuri, C.Y. Kong, N. Murooka, S. Kagei, Ind. Eng. Chem. Res. 39 (2000) 4462-4469.
- 208 [16] T. Funazukuri, C.Y. Kong, S. Kagei, Ind. Eng. Chem. Res. 41 (2002) 2812-2818.
- 209 [17] T. Funazukuri, C.Y. Kong, S. Kagei, Fluid Phase Equilib. 206 (2003) 163-178.
- 210 [18] T. Funazukuri, C.Y. Kong, S. Kagei, J. Supercrit. Fluids 27 (2003) 85-96.
- 211 [19] T. Funazukuri, C.Y. Kong, T. Kikuchi, S. Kagei, J. Chem. Eng. Data 48 (2003) 684-688.
- 212 [20] T. Funazukuri, C.Y. Kong, S. Kagei, Fluid Phase Equilib. 219 (2004) 67-73.
- 213 [21] C.Y. Kong, N.R.W. Withanage, T. Funazukuri, S. Kagei, J. Chem. Eng. Data 50 (2005)
- 214 1635-1640.
- 215 [22] C.Y. Kong, N.R.W. Withanage, T. Funazukuri, S. Kagei, J. Supercrit. Fluids 37 (2006) 63-71.
- 216 [23] C.Y. Kong, M. Mori, T. Funazukuri, S. Kagei, Anal. Sci. 22 (2006) 1431-1436.
- 217 [24] C. Pizarro, O. Suárez-Iglesias, I. Medina, J.L. Bueno, J. Chromatogr. A 1167 (2007) 202-209.
- 218 [25] T. Funazukuri, C.Y. Kong, S. Kagei, J. Supercrit. Fluids 46 (2008) 280-284.
- 219 [26] C. Pizarro, O. Suárez-Iglesias, I. Medina, J.L. Bueno, J. Supercrit. Fluids 43 (2008) 469-476.
- 220 [27] O. Suárez-Iglesias, I. Medina, C. Pizarro, J.L. Bueno, J. Chem. Eng. Data 53 (2008) 779-784.
- 221 [28] C. Pizarro, O. Suárez-Iglesias, I. Medina, J.L. Bueno, J. Supercrit. Fluids 48 (2009) 1-8.
- 222 [29] C. Pizarro, O. Suárez-Iglesias, I. Medina, J.L. Bueno, J. Chem. Eng. Data 54 (2009)
- 223 1467-1471.
- 224 [30] C.Y. Kong, M. Nakamura, K. Sone, T. Funazukuri, S. Kagei, J. Chem. Eng. Data 55 (2010)
- 225 3095-3100.
- 226 [31] C.Y. Kong, Y.Y. Gu, M. Nakamura, T. Funazukuri, S. Kagei, Fluid Phase Equilib. 297 (2010)

227 162-167.

228 [32] S.B. Kiselev, J.F. Ely, I.M. Abdulagatov, M.L. Huber, *Ind. Eng. Chem. Res.* 44 (2005)

229 6916-6927.

230 [33] T. Funazukuri, N. Nishimoto, N. Wakao, *J. Chem. Eng. Data* 39 (1994) 911-915.

231 [34] M. Toriumi, R. Katooka, K. Yui, T. Funazukuri, C.Y. Kong, S. Kagei, *Fluid Phase Equilib.* 297

232 (2010) 62-66.

233 [35] T. Funazukuri, Y. Ishiwata, *Fluid Phase Equilib.* 164 (1999) 117-129.

234

235 Figure captions

236 Fig. 1. Wavelength dependence on (a) absorbance of the peak top of a response curve A_{\max} , (b)
237 $A_{\max}/(u_0 \times \text{peak area})$, (c) D_{12} and (d) ε for phenylbutazone in supercritical CO_2 at 313.15 K
238 and 11.00 MPa measured by the CIR method.

239 Fig. 2. Effects of the secondary flow on (a) D_{12} and (b) ε measured at 240 nm, 313.15 K and 11.00
240 MPa for phenylbutazone in supercritical CO_2 by the CIR method.

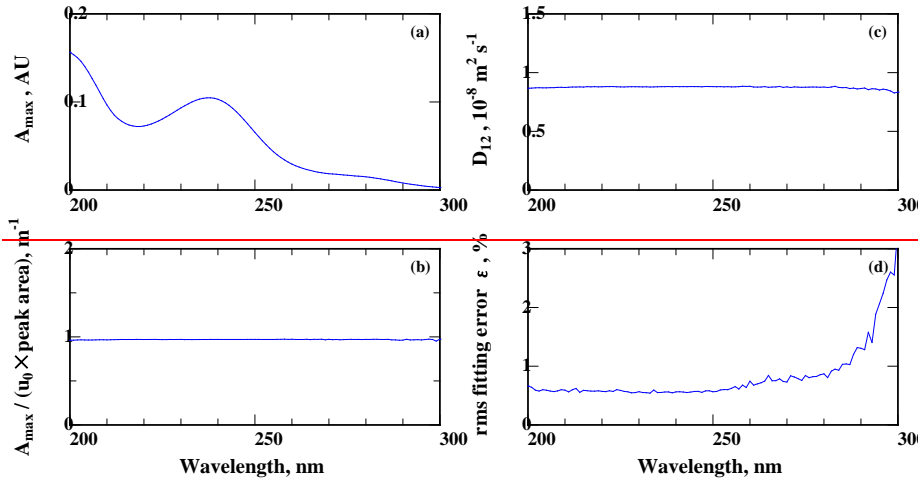
241 Fig. 3. Effects of the injected amount m of phenylbutazone in supercritical CO_2 at 240 nm, 313.15
242 K and 11.00 MPa on (a) absorbance of the peak top of a response curve A_{\max} , (b) $u_0 \times (\text{peak}$
243 $\text{area})$, (c) D_{12} and (d) ε measured by the CIR method.

244 Fig. 4. Pressure dependence on D_{12} of phenylbutazone measured by the CIR method in supercritical
245 CO_2 at 308.15 K (\circ), 313.15 K (\triangle), 318.15 K (\blacktriangle), 323.15 K (\square), 333.15 K (∇), 343.15 K
246 (\diamond) and at 8.50 to 40.00 MPa and together with the predicted values by Eq. (3) (solid line)

247 Fig. 5. Temperature dependence on D_{12} of phenylbutazone measured by the Taylor dispersion
248 method in ethanol at 298.15 K (\square), 303.15 K (∇), 308.15 K (\diamond), 313.15 K (\circ), 318.15 K
249 (\triangle), 323.15 K (\blacksquare), 328.15 K (\blacktriangledown), 333.15 K (\blacklozenge) and at atmospheric pressure.

250 Fig. 6. D_{12}/T vs. fluid viscosity η for all D_{12} data of phenylbutazone measured by the CIR method
251 in supercritical CO_2 and by the Taylor dispersion method in ethanol. The key is the same as
252 in Fig. 4 and Fig. 5, and (—) represented by Eq. (5).

253



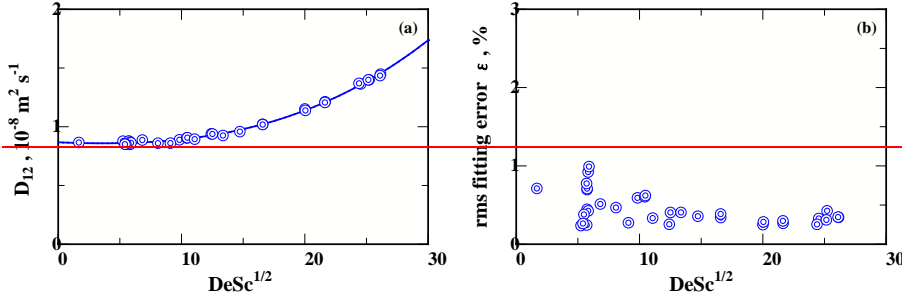
290

291

292

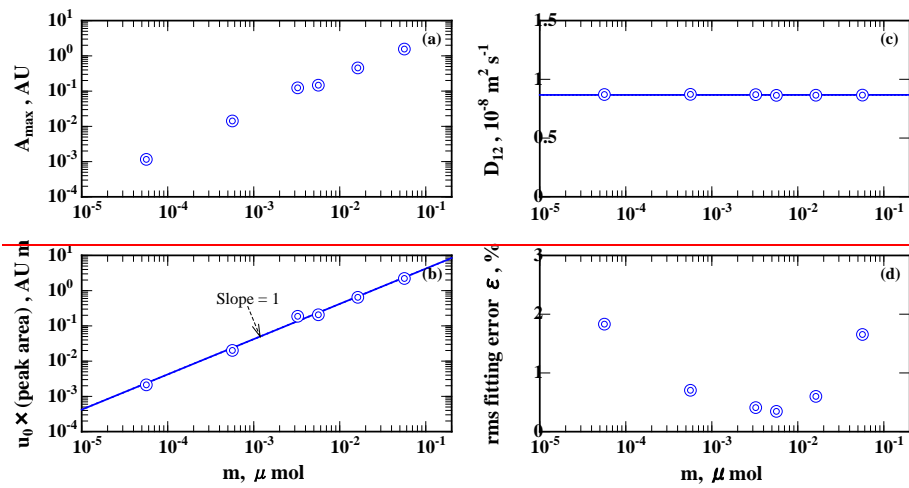
293

Fig. 1



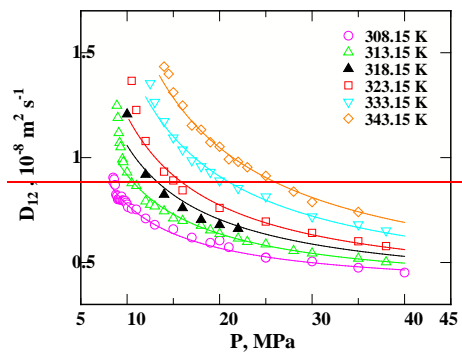
294
295
296
297

Fig. 2



298
299
300
301

Fig-3



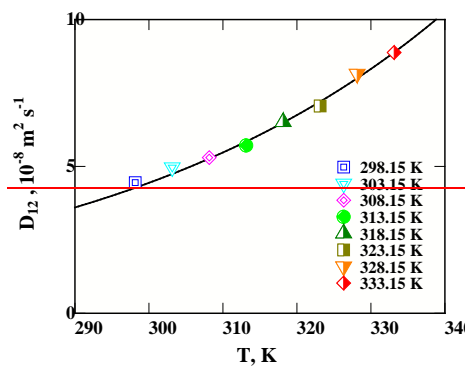
302

303

304

305

Fig. 4



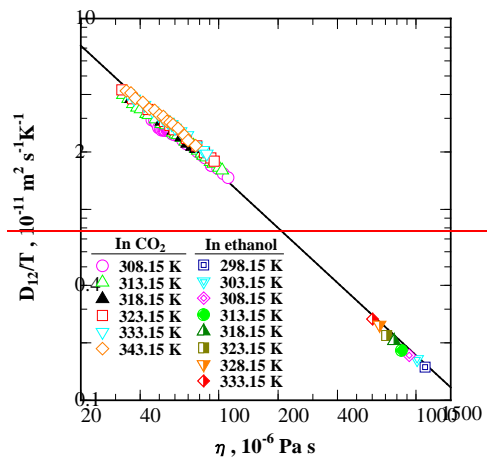
306

307

308

309

Fig-5



310

311

312

313

Fig. 6

254	List of the Tables
255	
256	Table 1
257	Diffusion coefficients D_{12} of phenylbutazone in supercritical CO ₂ measured by the CIR method at
258	308.15 to 343.15 K
259	
260	
261	Table 2
262	Diffusion coefficients D_{12} of phenylbutazone in ethanol measured by the Taylor dispersion method
263	at atmospheric pressure

Table 1

Diffusion coefficients D_{12} of phenylbutazone in supercriticalCO₂ measured by the CIR method at 308.15 to 343.15 K

308.15 K			
P (MPa)	ρ (kg m ⁻³)	η (10 ⁻⁶ Pa s)	D_{12} (10 ⁻⁸ m ² s ⁻¹)
8.50	612.12	45.87	0.905
8.60	625.37	47.26	0.897
8.70	636.50	48.46	0.870
8.80	646.10	49.52	0.824
8.90	654.56	50.48	0.817
9.00	662.13	51.36	0.801
9.10	668.99	52.17	0.804
9.20	675.28	52.92	0.800
9.30	681.07	53.63	0.799
9.40	686.46	54.29	0.815
9.50	691.50	54.92	0.797
9.60	696.24	55.52	0.796
9.70	700.71	56.10	0.792
9.80	704.95	56.65	0.794
9.90	708.97	57.17	0.786
10.00	712.81	57.68	0.777
10.10	716.48	58.18	0.764
10.50	729.76	60.00	0.756
11.00	743.95	62.03	0.753
12.00	767.07	65.51	0.710

13.00	785.70	68.50	0.680
15.00	815.06	73.57	0.659
17.00	838.09	77.90	0.619
19.00	857.21	81.76	0.594
20.00	865.72	83.56	0.605
21.00	873.67	85.29	0.573
25.00	901.23	91.69	0.524
25.00	901.23	91.69	0.523
30.00	929.11	98.86	0.505
35.00	952.29	105.42	0.475
40.00	972.26	111.57	0.452

313.15 K

P (MPa)	ρ (kg m ⁻³)	η (10 ⁻⁶ Pa s)	D_{12} (10 ⁻⁸ m ² s ⁻¹)
8.90	458.03	32.72	1.248
9.00	485.50	34.77	1.190
9.10	510.38	36.75	1.118
9.20	532.04	38.56	1.071
9.30	550.54	40.17	1.050
9.50	580.01	42.90	0.993
9.60	591.97	44.05	0.979
10.00	628.61	47.81	0.930
10.50	660.15	51.33	0.879
11.00	683.52	54.11	0.866
12.00	717.76	58.52	0.792
12.50	731.20	60.37	0.776

13.00	743.04	62.05	0.768
14.00	763.27	65.06	0.745
15.00	780.23	67.73	0.711
16.00	794.90	70.16	0.699
18.00	819.51	74.48	0.676
19.00	830.09	76.45	0.654
20.00	839.81	78.32	0.637
22.00	857.20	81.82	0.615
23.00	865.07	83.47	0.599
25.00	879.49	86.62	0.587
28.00	898.53	91.04	0.556
30.00	909.89	93.83	0.544
35.00	934.81	100.37	0.519
38.00	947.93	104.07	0.502

318.15 K

P (MPa)	ρ (kg m ⁻³)	η (10 ⁻⁶ Pa s)	D_{12} (10 ⁻⁸ m ² s ⁻¹)
10.00	498.25	36.01	1.207
12.00	657.74	51.25	0.919
14.00	720.47	59.06	0.824
16.00	759.98	64.71	0.760
18.00	789.24	69.34	0.704
20.00	812.69	73.36	0.679
22.00	832.36	76.97	0.661

323.15 K

P (MPa)	ρ (kg m ⁻³)	η (10 ⁻⁶ Pa s)	D_{12} (10 ⁻⁸ m ² s ⁻¹)
10.50	445.55	32.32	1.366
11.00	502.64	36.59	1.227
12.00	584.71	43.79	1.079
14.00	672.17	53.13	0.933
15.00	699.75	56.52	0.891
16.00	722.09	59.46	0.844
20.00	784.29	68.67	0.760
25.00	834.19	77.42	0.695
30.00	870.43	84.75	0.641
35.00	899.23	91.27	0.601
38.00	914.14	94.92	0.578

333.15 K

P (MPa)	ρ (kg m ⁻³)	η (10 ⁻⁶ Pa s)	D_{12} (10 ⁻⁸ m ² s ⁻¹)
12.50	471.52	34.66	1.354
13.00	505.35	37.27	1.265
14.00	561.37	42.05	1.173
15.00	604.09	46.13	1.095
16.00	637.50	49.61	1.038
17.00	664.59	52.65	0.986
18.00	687.25	55.35	0.958
19.00	706.68	57.79	0.931
20.00	723.68	60.04	0.890
22.00	752.38	64.07	0.854
25.00	786.55	69.33	0.814

30.00	829.71	76.82	0.719
35.00	862.94	83.34	0.681
38.00	879.83	86.96	0.652

343.15 K

P (MPa)	ρ (kg m ⁻³)	η (10 ⁻⁶ Pa s)	D_{12} (10 ⁻⁸ m ² s ⁻¹)
14.00	456.62	34.04	1.434
14.50	482.13	35.92	1.399
15.00	505.87	37.77	1.311
16.00	547.75	41.29	1.248
17.00	582.79	44.49	1.153
18.00	612.24	47.39	1.133
19.00	637.33	50.02	1.073
20.00	659.05	52.42	1.052
21.00	678.13	54.64	0.992
22.00	695.10	56.71	0.980
23.00	710.37	58.65	0.954
25.00	736.92	62.22	0.913
28.00	769.58	66.99	0.838
30.00	787.97	69.88	0.788
35.00	826.10	76.42	0.741

268

269

Table 2

Diffusion coefficients D_{12} of phenylbutazone in ethanol

measured by the Taylor dispersion method at atmospheric pressure

T (K)	ρ (kg m ⁻³)	η (10 ⁻⁶ Pa s)	D_{12} (10 ⁻¹⁰ m ² s ⁻¹)
298.15	785.48	1112.51	4.447
303.15	781.23	1012.64	4.966
308.15	776.93	923.93	5.300
313.15	772.56	844.89	5.713
318.15	768.13	774.28	6.512
323.15	763.62	711.01	7.057
328.15	759.03	654.18	8.152
333.15	754.36	602.99	8.878